A simple numerical model of a geometrically nonlinear Timoshenko beam

Chris Keijdener Andrei V. Metrikine
c.keijdener@tudelft.nl

Abstract

In the original problem for which this model was developed, one-dimensional flexible objects interact through a non-linear contact model. Due to the non-linear nature of the contact model, a numerical time-domain approach was adopted.

One of the goals was to see if the coupling between axial and transverse deformations had an influence on the results and so this capacity had to be included. In addition, large deformations should be allowed as well as non-prismatic, non-symmetrical cross-sections and inhomogeneous constitutive properties. To accommodate these requirements the linear model which was being used, was upgrade to meet these requirements.

The model created with the procedure explain in this paper consist of discrete masses connected by a set of nonlinear springs. The expressions for the masses and springs are obtained by discretization of the continuum representation of a Timoshenko beam. The required number of springs is proportional to the desired order of geometrical nonlinearity the model should accurately capture.

This paper explains the procedure to create a model which can accurately capture geometrically nonlinear effects up to a desired order..

1 Introduction

While studying the interaction between level ice and a downward sloping structures, the question arose whether axial deformation and buckling had an effect on the breaking length of the ice. To investigate this, the linear discrete element model of a Timoshenko beam was improved so that it could accurately capture geometrically nonlinear (GN) effects as well as non-prismatic, non-symmetrical cross-sections and inhomogeneous constitutive properties.

The linear model used falls in the category of discrete models whose origin is generally credited to [4] whom introduced the framework method to solve the plane stress problem. The earliest derivation found of a discrete system which accurately captures a Timoshenko beam was done by [3]. These models have been applied to study cracked beams [1] and moving loads [9].

In all works listed above, the authors assumed an element layout (the number of springs and their geometry) which involves some level of judgment and trial and error to obtain an element layout which can be matched to the continuum. The

matching results in expressions for the parameters of the discrete model, such as the springs stiffness and their geometry, in terms of quantities of the continuum such as the area, Youngs modules or density. In this paper we take the more traditional approach by directly discretizing a continuum. A consequence of directly discretizing the continuum, is that the element layout is obtained as a result of the derivation rather than a starting point like it was in previous works. The linear models and their element geometries can be obtained by linearizing the GN models derived in this paper.

In the first part of this paper the procedure is derived for obtaining discrete models which can accurately capture GN effects up to a given order. Next, using this procedure, the simplest possible model is created and is used to validate the procedure.

2 The discrete element

In this paper we start with the kinematic assumptions as defined in [6, 7]:

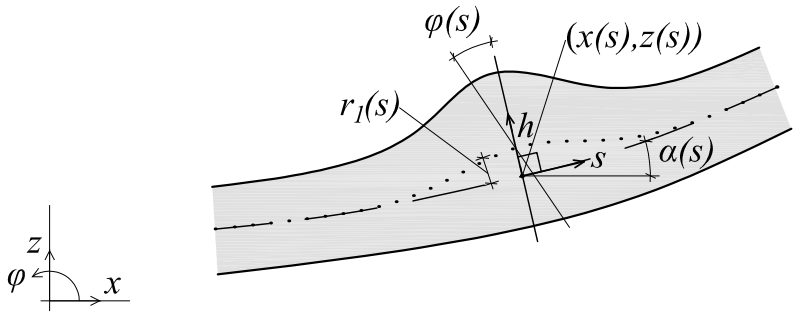

Figure 1: A non-prismatic, non-symmetric beam. The dashed line is the chosen reference axis while the dotted line is the neutral axis of the cross-section. The distance r_1 is the offset between the two. For beams with a cross-section which is symmetric with respect to its neutral axis, r_1 will be zero for all elements. However, for non-symmetric beams r_1 will be none zero and vary along the length. The coordinate s runs along the chosen reference axis and the coordinate h runs tangential to it.

To ensure that the deflections of the beam reside in the x,z-plane, the cross-section and loading are assumed to be symmetric with respect to this plane. From this continuous beam a piece is cut with a length l. The potential energy of this piece is:

$$\begin{aligned} \mathbb{V}_{\text{piece},\varepsilon} &= \frac{1}{2}\int_{s_n-l/2}^{s_n+l/2}\int_{A(s)} \sigma\,(s,h)\,\varepsilon\,(s,h)\;\mathrm{d}A\;\mathrm{d}x \\ \mathbb{V}_{\text{piece},\gamma} &= \frac{1}{2}\int_{s_n-l/2}^{s_n+l/2}\int_{A(s)} \tau\,(s,h)\,\gamma\,(s,h)\;\mathrm{d}A\;\mathrm{d}x \end{aligned} \tag{1}$$

where s_n is the midpoint of the piece, σ is the normal stress, ϵ is the normal strain, τ is the shear stress and γ is the shear strain and all the constitutive properties are

allowed to be a function of s. This continues piece is now discretized using finite differences. In this paper a two-point discretization scheme is used for simplicity, resulting in a linear element as can be seen in the figure below.

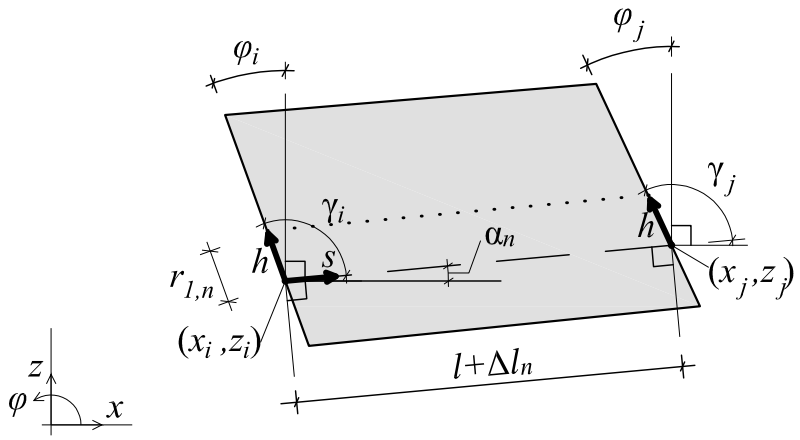

Figure 2: The element n which is part of a Timoshenko beam and connects nodes i and j.

Due to the presence of two nodes per element, the following expressions relate the continuum and the discrete element:

$$x_j - x_i = l \left.\frac{\partial x(s)}{\partial s}\right|_{s=s_n} + O(l), \quad \frac{x_j + x_i}{2} = x(s)|_{s=s_n} + O\left(l^2\right) \tag{2}$$

In these equations the x-displacement was used but the same relations apply to any property which is a function of s, such as $z(s,h)$ or $\gamma(s,h)$. These relations also show that for all s-dependent constitutive properties, the value half-way the element should be used, again resulting in a second order error in their discretization. This will be denoted with a subscript n, so for instance E_n stand for $E(s)|_{s=s_n}$. This discretization also requires the inhomogeneous or non-prismatic nature of the beam to be smooth so that higher order derivatives with respect to s are small.

After discretization the integral over s becomes trivial as all s-dependencies have been removed and so the expression for the potential energy (Eq. (1)) of the discrete element becomes:

$$\begin{aligned} \mathbb{V}_{n,\varepsilon} &= \frac{l}{2} \int_{A_n} \sigma_n(h)\, \varepsilon_n(h)\, dA \\ \mathbb{V}_{n,\gamma} &= \frac{l}{2} \int_{A_n} \tau_n(h)\, \gamma_n(h)\, dA \end{aligned} \tag{3}$$

where σ_n, ϵ_n, τ_n and γ_n are the stresses and strains of the element. These will be defined in the next section which covers to potential energy of the element. The kinetic energy is discussed afterwards.

2.1 Potential energy

The following geometrical relations apply the element shown in Figure 2 (note that all coordinates are global):

$$\begin{aligned}
\hat{x}_i(h) &= x_i + (h + r_{1,n})\cos(\varphi_i + \pi/2) = x_i - (h + r_{1,n})\sin(\varphi_i) \\
\hat{z}_i(h) &= z_i + (h + r_{1,n})\sin(\varphi_i + \pi/2) = z_i + (h + r_{1,n})\cos(\varphi_i) \\
\hat{x}_j(h) &= x_j - (h + r_{1,n})\sin(\varphi_j) \\
\hat{z}_j(h) &= z_j + (h + r_{1,n})\cos(\varphi_j)
\end{aligned} \tag{4}$$

Similarly to what is done in infinitesimal strain theory, [8] the normal and shear strains are defined using the relations in Eq. (4):

$$\varepsilon_n(h) = \frac{l_n(h) - l}{l} = \frac{\Delta l_n(h)}{l} = \frac{1}{l}\left(\sqrt{\Delta X_n^2(h) + \Delta Z_n^2(h)} - l\right) \tag{5}$$

$$\begin{aligned}
-\gamma_n(h) &= \frac{\gamma_i(h) + \gamma_j(h)}{2} - \frac{\pi}{2} - \gamma_{0,n} \\
&= \frac{1}{2}\left(\left(\varphi_i + \frac{\pi}{2}\right) - \alpha_n(h) + \left(\varphi_j + \frac{\pi}{2}\right) - \alpha_n(h)\right) - \frac{\pi}{2} - \gamma_{0,n} \\
&= \frac{\varphi_i + \varphi_j}{2} - \alpha_n(h) - \gamma_{0,n} = \varphi_n - \alpha_n(h) - \gamma_{0,n} \\
&\rightarrow \gamma_n(h) = \alpha_n(h) - \varphi_n + \gamma_{0,n}
\end{aligned} \tag{6}$$

$$\begin{aligned}
\alpha_n(h) &= \arctan\left(\frac{\Delta Z_n(h)}{\Delta X_n(h)}\right) \\
\Delta X_n(h) &= \hat{x}_j(h) - \hat{x}_i(h),\ \Delta Z_n(h) = \hat{z}_j(h) - \hat{z}_i(h)
\end{aligned} \tag{7}$$

where l_n is the current length of the element, Δl_n is the elongation of the element, γ_n is the shear angle of the element where $-\pi/2$ subtracts the default shear angle which account for the fact that by default the cross-section is perpendicular to the beam axis and $\gamma_{0,n}$ accounts for any non-zero shear angle in the undeformed state, Δx_n and Δz_n are the distance between the two nodes in their respective direction and is the undeformed length (element size) given by $L(N+1)$ where L is the length of the beam and N is the total number of elements.

Next the following linear stress-strain relations are assumed:

$$\begin{aligned}
\sigma_n &= E_n \varepsilon_n(h) = \frac{E_n}{l}\Delta l_n(h) \\
\tau_n &= G_n \gamma_n(h)
\end{aligned} \tag{8}$$

Usage of nonlinear materials is also possible as long as both stresses remain uncoupled. Using these relations, the potential energy of the element becomes:

$$\begin{aligned}
\mathbb{V}_{n,\varepsilon} &= \frac{l}{2}\int_{A_n} \frac{E_n}{l^2}\Delta l_n^2(h)\ \mathrm{d}A \\
\mathbb{V}_{n,\gamma} &= \frac{l}{2}\int_{A_n} G_n \gamma_n^2(h)\ \mathrm{d}A
\end{aligned} \tag{9}$$

The next step is to solve the two cross-sectional integrals.

2.2 Solving the cross-sectional integrals

Due to the complexity of the expressions for the elongations, analytically solving the cross-sectional integrals (CSI) in Eq. (9) results in so many terms that it makes evaluation impractically slow. Because of this, we seek to find an approximate system for which the integral can be solved, whose error compared to the exact solution of the CSI is acceptable. The first step in finding this approximate system is to investigate a Taylor series expansion (TSE) of the squared strains. The TSE is done for an element which is part of a beam whose undeformed shape is a straight line and which is not subjected to any pre-stress. The approximate system will prove to be independent of these two assumptions. The TSE of the element can be written in the following form:

$$\begin{aligned}\mathbb{V}_{n,\varepsilon} &= \frac{l}{2}\frac{E_n}{l^2}\int_{A_n} B_{n,0}h^0 + B_{n,1}h^1 + B_{n,2}h^2 + .. + B_{n,\infty}h^\infty \\ \mathbb{V}_{n,\gamma} &= \frac{l}{2}G_n\int_{A_n} C_{n,0}h^0 + C_{n,1}h^1 + C_{n,2}h^2 + .. + C_{n,\infty}h^\infty\end{aligned} \tag{10}$$

where the coefficients B_0 and C_0 contain all terms which are proportional to h^0 of their respective strain and so on. The order of h-dependency goes up to infinity because the normal strain contains a square root and the shear strain an arctangent.

Because the strains were assumed to be constant over the width of the beam, the CSI is only dependent on h. Looking at Eq. (8) however, these h-dependencies are all multiplications with a certain order of h. These simple dependencies on h allow the CSIs to be calculated in a trivial manner if two assumption are made: 1) that the elasticity of the material is uniform over the cross-section and 2) that all terms which result from the TSE have the same profile over the height as the strain they originate from. This implies that higher order strain components, for instance say those in $B_{n,5}$, have the same profile as the normal strain they originates from, which is a linear profile. Under these assumptions the integral in Eq. (10) evaluates to:

$$\begin{aligned}\mathbb{V}_{n,\varepsilon} &= \frac{l}{2}\frac{E_n}{l^2}\int_{A_n} B_{n,0}h^0 + B_{n,1}h^1 + B_{n,2}h^2 + .. + B_{n,\infty}h^\infty \\ \mathbb{V}_{n,\gamma} &= \frac{l}{2}G_n\int_{A_n} C_{n,0}h^0 + C_{n,1}h^1 + C_{n,2}h^2 + .. + C_{n,\infty}h^\infty\end{aligned} \tag{11}$$

Both equations contain infinitely many terms. However, if this expansion is truncated at a certain order ϖ, which then defines the *maximum order of geometrical nonlinearity* of the discrete system, the expansion only contains a finite number of orders:

$$\begin{aligned}\mathbb{V}^{(\varpi)}_{n,\varepsilon} &= \frac{l}{2}\frac{E_n}{l^2}\left(A_nB_{n,0} + A_nr_{1,n}B_{n,1} + I_nB_{n,2} + .. + A_nr_{\varpi,n}B_{n,\varpi}\right) \\ \mathbb{V}^{(\varpi)}_{n,\gamma} &= \frac{l}{2}G_n\left(\kappa_{0,n}A_nC_{n,0} + \kappa_{1,n}A_nr_{1,n}C_{n,1} + \kappa_{2,n}I_nC_{n,2} + .. + \kappa_{\varpi,n}A_nC_{n,\varpi}\right)\end{aligned} \tag{12}$$

The order of GN of a term in the expansion is defined as the total number of s-dependent variables in that term. The relation between the total number of unique solutions to the CSIs and ϖ is shown in the table below:

	$\varpi = 1$	$\varpi = 2$	$\varpi = 3$	$\varpi = 4$	$\varpi = 5$	$\varpi = 6$
ϵ_n	3	3	3	4	5	6
γ_n	1	2	3	4	5	6

Table 1: The total number of unique solutions to the CSI for different orders of GN (ϖ) for both strains

To give an example, the 3 unique solutions to the CSIs in the potential energy of ϵ_n truncated at $\varpi = 1$ are A_n, $A_n r_{1,n}$ and I_n. Apart from an anomaly in the lower orders of the normal strain, there is a linear relation between ϖ and the highest order of ϖ-dependency in the CSIs. This relation forms the basis of the approximation of the CSIs. If the discrete system is only required to be accurate up to a certain order ϖ, the number of solutions to the CSIs is finite. To ensure that the approximate system can accurately capture all GN effects up to order ϖ, a solution is sought in the following form which is based on Eq. (9):

$$\begin{aligned} \hat{\mathbb{V}}_{n,\varepsilon}^{(\varpi)} &= \frac{l}{2} \int_{A_n} \frac{E_n}{l^2} \sum_{q=1}^{Q_\varepsilon} k_{n,q} \Delta l_n^2 \left(h = h_{n,q}\right) \, dA \\ \hat{\mathbb{V}}_{n,\gamma}^{(\varpi)} &= \frac{l}{2} \int_{A_n} G_n \sum_{q=1}^{Q_\gamma} g_{n,q} \gamma_n^2 \left(h = \eta_{n,q}\right) \, dA \end{aligned} \tag{13}$$

where $k_{n,q}$ and $g_{n,q}$ are unknown dimensionless scaling factors, $h_{n,q}$ and $\eta_{n,q}$ are unknown offsets of the springs with respect to the chosen reference axis and Q_ϵ and Q_γ are the total number of springs. The evaluation of the strains at a specific offset ($h_{n,q}$ and $\eta_{n,q}$) effectively turns the continuously distributed elasticity into a discrete spring with a certain offset, visualized below.

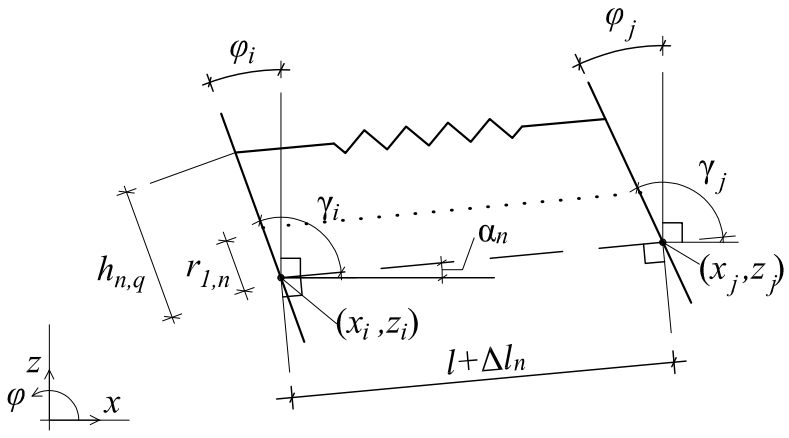

Figure 3: The continuously distributed normal strain has been replaced by a spring with a certain offset $h_{n,q}$. The same applies to the shear strain.

This means that the integral over the cross-section has been replaced by a summation of springs, each with an unknown scale and offset. To understand the implications of this approximation, the truncated TSE of the approximate form (Eq.

(11)) and the exact form (Eq. (13)) are compared (the exact same can be for the shear energy):

$$\begin{aligned}\mathbb{V}_{n,\varepsilon}^{(\varpi)} &= \frac{l}{2}\frac{E_n A_n}{l^2}\left(B_{n,0} + r_1 B_{n,1} + .. + r_\varpi B_{n,\varpi}\right)\\ \hat{\mathbb{V}}_{n,\varepsilon}^{(\varpi)} &= \frac{l}{2}\frac{E_n A_n}{l^2}\sum_{q=1}^{Q_\varepsilon} k_{n,q}\left(\hat{B}_{n,0} h_{n,q}^0 + \hat{B}_{n,1} h_{n,q}^1 + .. + \hat{B}_{n,\varpi} h_{n,q}^\varpi\right)\end{aligned} \tag{14}$$

At this point it is important to understand how the approximation differs from the exact solution, but, more importantly, how they are similar. Because the strain equation for each spring is based on those of the continuously distributed strain, their TSE will be exactly the same apart from their dependence on h. This means that for any given state of the elements the strain components which are contained in their respective TSE will be exactly the same. This means that $B_0 = \hat{B}_0$ and $C_0 = \hat{C}_0$ and the same holds for all other orders. The different dependence on h results in a different type of solution to the CSIs: for the continuum the integral actually integrates over different orders of h while the approximate system has become independent of h due to the substitution and so the integral evaluates to A_n for all terms. However, as the approximate system still has two unknowns per spring, the two equations in Eq. (14) can be matched, so that the CSI of both systems ends up being the same. This results in the following set of equations:

$$\begin{cases} \sum_{q=1}^{Q_\varepsilon} k_{n,q} h_{n,q}^0 = 1 \\ \sum_{q=1}^{Q_\varepsilon} k_{n,q} h_{n,q}^1 = r_{1,n} \\ \dots \\ \sum_{q=1}^{Q_\varepsilon} k_{n,q} h_{n,q}^\varpi = r_{\varpi,n} \end{cases}, \quad \begin{cases} \sum_{q=1}^{Q_\gamma} g_{n,q} \eta_{n,q}^0 = \kappa_{0,n} \\ \sum_{q=1}^{Q_\gamma} g_{n,q} \eta_{n,q}^1 = \kappa_{1,n} \\ \dots \\ \sum_{q=1}^{Q_\gamma} g_{n,q} \eta_{n,q}^\varpi = \kappa_{\varpi,n} \end{cases} \tag{15}$$

where $r_{0..\varpi,n} = 1/A_n \int_{A_n} h^{0..\varpi}\, dA$, $\kappa_{0,n}$ is the Timoshenko shear correct factor and $\kappa_{1..\varpi,n}$ are its higher order equivalents. The right hand side of both sets are different as the continuous normal and shear strains have a different distribution along the height. The total number of equations to be satisfied is equal to the number of unique solutions to the CSIs, which was shown in Table 1. Each spring has a total of two unknowns: its offset and scaling factor. Since the same number of unknown is needed as their are equations, the required number of springs (Q_ϵ and Q_γ) becomes:

$$Q_\varepsilon = \max\left(\lceil \varpi/2 \rceil, 2\right),\ Q_\gamma = \lceil \varpi/2 \rceil \tag{16}$$

where the brackets indicate the ceiling function and the minimum of two normal springs is due to linear bending effects being proportional to I_n.

With all the unknowns determined the discrete element can accurately capture the potential energy up to the specified order of geometrical nonlinearity ϖ. This

means that the resulting discrete element is not an exact solution to the CSI and thus will have an error compared to that exact solution. This error is independent of the mesh size and manifests itself as an incorrect solution to the CSIs for orders higher than ϖ. The error can be reduced by increasing ϖ but for a given order of ϖ there will be a non-converging error. Note that higher order (in terms of h) CSIs are also multiplied with higher order (in terms of ϖ) strain components. The error in the incorrect solution to the CSI is therefore only as important as the magnitude of the strain component it is multiplied with. As the influence on the solution (displacements, stresses, etc.) diminishes as the order of the strain components increases, the influence of the error to the CSI also diminishes.

The final item to consider is the state which was used to perform the TSE and whether this has any influence on the matching process. A different state does result in a different TSE of the potential energies but can always be rewritten in the form show in Eq. (10). The strain components contained in $B_{n,0..\infty}$ and $C_{n,0..\infty}$ will be different they will still be equal to $\hat{B}_{n,0..\infty}$ and $\hat{C}_{,0..\infty}$ since both are based on the same strain equations. This means that the matching process is independently of the state used for the TSE. The absolute value of the non-converging error will be slightly different for each state, as in each state the importance of higher order is slightly different. However, in general the importance of higher orders is small and so the overall magnitude of the non-converging error will be independent of the state of the system.

This ends the discretization of the potential energy. The next step is to consider the kinetic energy.

2.3 Kinetic energy

The kinetic energy requires the velocities. Based on Eq. (2) the expressions for the velocities of the element are:

$$\begin{aligned}\dot{\hat{x}}_n &= \frac{\partial\left(\hat{x}_i+\hat{x}_j\right)/2}{\partial t} = \frac{1}{2}\left(\dot{x}_i-\left(h+r_1\right)\cos\left(\varphi_i\right)\dot{\varphi}_i+\dot{x}_j-\left(h+r_1\right)\cos\left(\varphi_j\right)\dot{\varphi}_j\right)\\ \dot{\hat{z}}_n &= \frac{\partial\left(\hat{z}_i+\hat{z}_j\right)/2}{\partial t} = \frac{1}{2}\left(\dot{z}_i-\left(h+r_1\right)\sin\left(\varphi_i\right)\dot{\varphi}_i+\dot{z}_j-\left(h+r_1\right)\sin\left(\varphi_j\right)\dot{\varphi}_j\right)\end{aligned} \tag{17}$$

Using these relations the kinetic energy of an element becomes:

$$\mathbb{T}_n = \frac{l}{2}\int_A \rho\left(\dot{\hat{x}}_n^2+\dot{\hat{z}}_n^2\right)\,dA \tag{18}$$

Luckily, the expressions for the velocities are much simpler than those of the strains and so the CSI can be solved analytically under the assumption that the density is uniform over the cross-section:

$$\begin{aligned}\mathbb{T}_n &= \frac{J_n}{8}\left(\left(-\cos\left(\varphi_i\right)\dot{\varphi}_i-\cos\left(\varphi_j\right)\dot{\varphi}_j\right)^2+\left(-\sin\left(\varphi_i\right)\dot{\varphi}_i-\sin\left(\varphi_j\right)\dot{\varphi}_j\right)^2\right)\\ &+\frac{m_n}{4}\left(\dot{x}_i-r_{1,n}\cos\left(\varphi_i\right)\dot{\varphi}_i+\dot{x}_j-r_{1,n}\cos\left(\varphi_j\right)\dot{\varphi}_j\right)^2\\ &+\frac{m_n}{4}\left(\dot{y}_i-r_{1,n}\sin\left(\varphi_i\right)\dot{\varphi}_i+\dot{y}_j-r_{1,n}\sin\left(\varphi_j\right)\dot{\varphi}_j\right)^2\end{aligned} \tag{19}$$

where $J_n = \int_{A_n} \rho_n h^2 l \, dA = \rho_n l \, (I_n + r_{1,n} A_n)$ and $m_n = \int_{A_n} \rho_n l \, dA = \rho_n A_n l$. With this, both the kinetic and potential energy of the discrete element have been defined and so the Lagrangian of the system if known.

Finally, to avoid numerical issues the arctan2 function should be used when computing the shear angle γ_n. In addition, the vector containing the shear angle of all elements can contain jumps of 2π because the range of α_n is limited to the range of the arctan2 ($[-\pi, \pi]$) while γ_n does not have this limitation. These jumps should be removed from the vector.

3 Model validation

This chapter will validate the methodology derived in this paper. The first step is to create a model. The model is then validated against solutions found in the literature.

3.1 Creating a simple beam model

The only step to be done in creation of the model is to perform is matching in Eq. (15). To perform the matching, the order of GN of the model has to be set. ϖ is set to 1 as this results in the fastest model possible and its performance is already sufficiently accurate.

To further simplify the model, the anomaly visible in Table 1 is investigated to see which terms are proportional to I_n as those are the once which necessitate the second axial spring. An investigation shows that the anomaly is caused by linear bending effects, e.g $\int_A E z^2 \phi_{xx} \, dA = EI\phi_{xx}$. This strain component could be capture by the second axial spring, as previously suggested, but can also be captured by a rotational spring. As the rotational spring is faster, we opt for that solution. This results in the following set of equations, similar to Eq. (15):

$$\begin{cases} k_n h_n^0 = 1 \\ k_n h_n^1 = r_{1,n} \end{cases}, \quad \begin{cases} g_n \eta_n^0 = \kappa_{0,n} \\ g_n \eta_n^1 = \kappa_{1,n} = \kappa_{0,n} r_{1,n} \end{cases}, \quad \begin{cases} \frac{l}{2} k_{n,\mathrm{rot}} = \frac{l}{2} \frac{E_n I_n}{l^2} \end{cases} \tag{20}$$

where $k_{n,\mathrm{rot}}$ is the unknown stiffness of the rotational spring. This set of equations is readily solved. The equations of motion (EOMs) can now be obtained using the Euler-Lagrange equation. The EOMs were implemented in matlab at used to compute the results in the following section.

3.2 Validation

The model is now validated against solutions found in existing literature:

- Cantilever with small point load at the end (linear behavior): quadratic convergence
- Cantilever with large point load at the end (GN behavior) (from [2]): initial converges quadratically but then converges to a non-decaying error, see below:

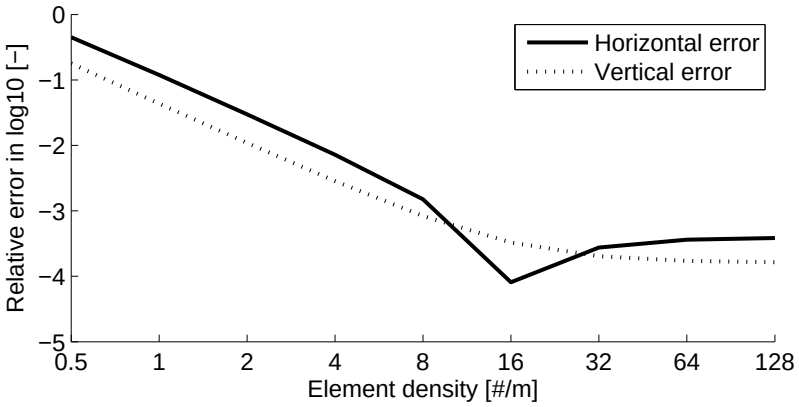

- GN cantilever with large moment causing the beam to roll up to a circle: exact (error is equal to the error of the Newton-Rapson scheme used to solve the nonlinear problem):

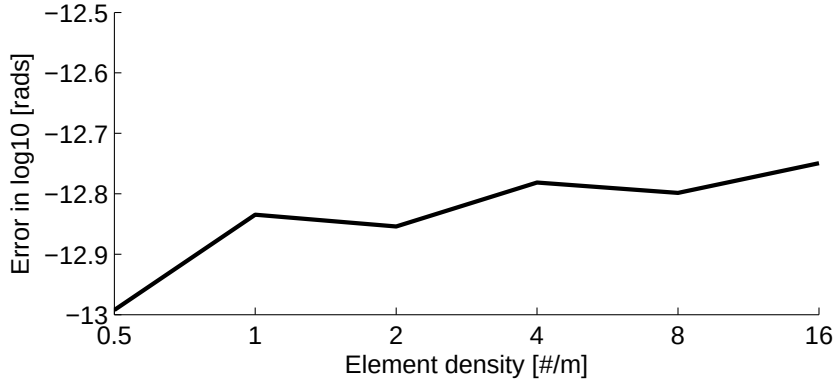

- Axial buckling: the converged predicted buckling load has an error of about 0.44 % when compared with the buckling load given by Eulers formula.

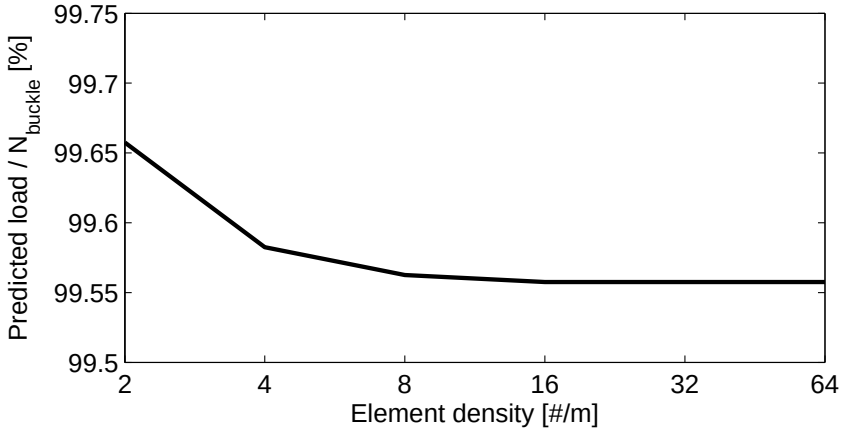

- Eigenfrequencies (from [2]): quadratic convergence
- GN cantilever with follower load (from [5]): good agreement, see below:

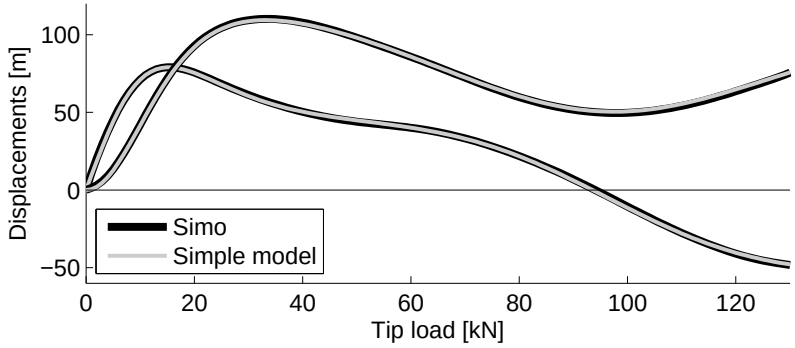

4 Conclusion

A simple way to derive a discrete model of a geometrically nonlinear Timoshenko beam has been presented. The model does not include warping effects and there are no compressive effects in transversal direction. However, for problems where these effects can be ignored, the results of the model are in good agreement with existing formulation. The relative ease at which the model can be implemented makes it ideal for educational purposes.

Acknowledgements

The authors wish to acknowledge the support from the Research Council of Norway through the Centre for Research-based Innovation SAMCoT and the support from all SAMCoT partners.

References

[1] Attar, M., Karrech, A., & Regenauer-Lieb, K. (2014). Free vibration analysis of a cracked shear deformable beam on a two-parameter elastic foundation using a lattice spring model. Journal of Sound and Vibration, 333, 23592377. doi:10.1016/j.jsv.2013.11.013

[2] Gerstmayr, J., Matikainen, M. K., & Mikkola, A. M. (2008). A geometrically exact beam element based on the absolute nodal coordinate formulation. Multibody System Dynamics, 20, 359384. doi:10.1007/s11044-008-9125-3

[3] Heinsbroek, A. G. T. J., & Blauwendraad, J. (1989). Reinforced concrete beams under shock loading, linear and nonlinear response. Heron, 34(3).

[4] Hrennikoff, A. (1941). Solution of Problems of Elasticity by the Frame-Work Method. Applied Scientific Research, A8, 169175.

[5] Simo, J. C., & Vu-Quoc, L. (1986). A three-dimensional finite-strain rod model. part II: Computational aspects. Computer Methods in Applied Mechanics and Engineering. doi:10.1016/0045-7825(86)90079-4

[6] Timoshenko, S. P. (1921). On the correction factor for shear of the differential equation for transverse vibrations of bars of uniform cross-section. Philosophical Magazine, 744.

[7] Timoshenko, S. P. (1922). On the transverse vibrations of bars of uniform cross-section. Philosophical Magazine, 125.

[8] Wikipedia. (2015). Geometric derivation of the infinitesimal strain tensor. Retrieved February 18, 2015, from http://en.wikipedia.org/wiki/Infinitesimal_strain_theory

[9] Yavari, A., Nouri, M., & Mofid, M. (2002). Discrete element analysis of dynamic response of Timoshenko beams under moving mass. Advances in Engineering Software, 33(3), 143153. doi:10.1016/S0965-9978(02)00003-0

Chris Keijdener, Stevinweg 1, 2628 CN Delft, The Netherlands
Andrei V. Metrikine, Stevinweg 1, 2628 CN Delft, The Netherlands